Article

Synthesis, Antibacterial Activity, and Mechanisms of Novel 6-Sulfonyl-1,2,4-triazolo[3,4-b][1,3,4]thiadiazole Derivatives

Sikai Wu,[†] Jing Shi,[†] Jixiang Chen, Deyu Hu, Liansheng Zang,* and Baoan Song*

Read Online

ACCESS | Metrics & More | Article Recommendations | Supporting Information

ABSTRACT: A series of novel 6-sulfonyl-1,2,4-triazolo[3,4-b][1,3,4]thiadiazole derivatives were designed and synthesized. CoMFA models were established to analyze the quantitative structure−activity relationships on the basis of the EC_{50} values of the compounds. The models were used to design and synthesize compounds **32** and **33** with higher activities. The EC_{50} values of compound **33** against *Xanthomonas oryzae* pv. *oryzae* (*Xoo*) and *Xanthomonas oryzae* pv. *oryzicola* (*Xoc*) were 0.59 and 1.63 mg/L, respectively, which were higher than those of thiodiazole copper (90.43 and 97.93 mg/L) and bismerthiazol (68.37 and 75.59 mg/L). Moreover, protective activities of compound **33** against bacterial leaf streak (BLS) and bacterial leaf blight (BLB) were 49.65% and 49.42%, respectively, which were superior to those of thiodiazole copper (44.28% and 41.51%) and bismerthiazol (38.89% and 40.09%). Protective activity of compound **33** against BLS was closely related to the improvement of defense-related enzyme activities, chlorophyll content, and photosynthesis activation. This is consistent with the upregulated expression of defense responses and photosynthesis-related proteins.

KEYWORDS: sulfone derivatives, 1,2,4-triazolo[3,4-b][1,3,4]thiadiazole moiety, antibacterial activity, CoMFA models, mechanisms of action, label-free proteomic

INTRODUCTION

As a staple food for more than one-half of the world's population, rice is frequently exposed to the threats of bacterial diseases.[1,2] Among these diseases, bacterial leaf streak (BLS) and bacterial leaf blight (BLB), caused by *Xanthomonas oryzae* pv. *oryzicola* (*Xoc*) and *Xanthomonas oryzae* pv. *oryzae* (*Xoo*), are two serious bacterial diseases that can decrease the yield of rice up to 20−50%.[3−5] Currently, only a few traditional antibacterial agents, such as bismerthiazol (BT), thiodiazole copper (TC), and streptomycin, have been used to control bacterial diseases. However, their frequent and long-term use leads to increased resistance and poor control effects.[6,7] Therefore, there is an urgent need to discover new antibacterial agents to control bacterial diseases in rice.

In our previous works, many sulfonyl-substituted thiadiazole/oxadiazole compounds were prepared, and some target compounds showed good antibacterial activities.[8−12] Among these compounds, the candidate drug JHXJZ was found, and a compound introducing a flexible chain in the 2-position of JHXJZ showed higher antibacterial activity. However, in the previous design of the target compounds, we were limited to changing the substituents at positions 2 and 5 of 1,3,4-oxadiazole/thiadiazole and did not change the oxadiazole/thiadiazole scaffold. It is possible that changing the 1,3,4-oxadiazole/thiadiazole scaffold while keeping the sulfone group unchanged could result in highly effective antibacterial agents with novel structures. As a class of thiadiazole derivatives, 1,2,4-triazolo[3,4-b][1,3,4]thiadiazole compounds contain characteristics similar to those of thiadiazole. They often exhibit higher biological activity, especially antimicrobial activity, due to their thickening with a triazole.[13] 1,2,4-

Triazolo[3,4-b][1,3,4]thiadiazole compounds are widely used to develop medical antibacterial agents[14−17] and antifungal agents,[18−20] but they have been less studied in the control of plant pathogenic bacteria.

To find highly effective antibacterial agents with novel structures, on the basis of our previous work, we retained the sulfone group and introduced the triazolo[3,4-b][1,3,4]-thiadiazole ring instead of the 1,3,4-thiadiazole/oxadiazole ring. A series of 6-sulfonyl-1,2,4-triazolo[3,4-b][1,3,4]-thiadiazole derivatives were designed and synthesized (Figure 1), and their antibacterial activities were evaluated. Two CoMFA models were established to analyze their quantitative structure−activity relationship on the basis of the EC_{50} values of the compounds against *Xoo* and *Xoc*. On the basis of the CoMFA models, compounds **32** and **33**, which had higher antibacterial activities, were designed and synthesized. The in vivo antibacterial activities of compound **33** were evaluated against BLB and BLS under greenhouse conditions. In addition, the induced rice defense of compound **33** was investigated by determining the activities of defense-related enzymes, chlorophyll content, and differentially expressed proteins.
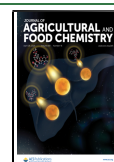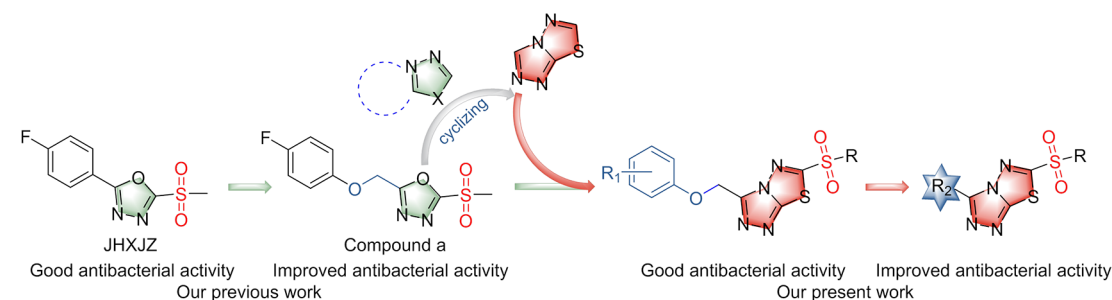
Figure 1. Design of target compounds.

Scheme 1. Synthesis Route of Target Compounds 1−33

1: R = (4-chlorophenoxy)methyl	R_1 = CH$_2$CH$_3$	**18:** R = CH$_3$	R_1 = 4-Cl-Benzyl
2: R = (4-chlorophenoxy)methyl	R_1 = CH$_2$CH$_2$CH$_3$	**19:** R = CH$_2$CH$_3$	R_1 = CH$_2$CH$_3$
3: R = (4-chlorophenoxy)methyl	R_1 = CH$_2$CH$_2$CH$_2$CH$_3$	**20:** R = CH$_2$CH$_3$	R_1 = CH$_2$CH$_2$CH$_3$
4: R = CH$_2$OCH$_3$	R_1 = CH$_2$CH$_3$	**21:** R = CH$_2$CH$_3$	R_1 = CH$_2$CH$_2$CH$_2$CH$_3$
5: R = CH$_2$OCH$_3$	R_1 = CH$_2$CH$_2$CH$_3$	**22:** R = CH$_2$CH$_3$	R_1 = CH$_2$-Cyclopropyl
6: R = CH$_2$OCH$_3$	R_1 = CH$_2$CH$_2$CH$_2$CH$_3$	**23:** R = CH$_2$CH$_3$	R_1 = CH$_2$-Cyclohexyl
7: R = CH$_2$OCH$_3$	R_1 = 4-CH$_3$-Benzyl	**24:** R = CH$_2$CH$_3$	R_1 = Benzyl
8: R = H	R_1 = CH$_2$CH$_2$CH$_2$CH$_3$	**25:** R = CH$_2$CH$_3$	R_1 = 4-CH$_3$-Benzyl
9: R = H	R_1 = CH$_2$CH = CH$_2$	**26:** R = CH$_2$CH$_3$	R_1 = 4-CH$_3$O-Benzyl
10: R = H	R_1 = 4-CH$_3$O-Benzyl	**27:** R = CH$_2$CH$_3$	R_1 = 4-Cl-Benzyl
11: R = CH$_3$	R_1 = CH$_2$CH$_3$	**28:** R = Cyclopropyl	R_1 = CH$_2$CH$_2$CH$_3$
12: R = CH$_3$	R_1 = CH$_2$CH$_2$CH$_3$	**29:** R = Cyclopropyl	R_1 = CH$_2$CH$_2$CH$_2$CH$_3$
13: R = CH$_3$	R_1 = CH$_2$CH$_2$CH$_2$CH$_3$	**30:** R = Cyclohexyl	R_1 = CH$_2$CH$_3$
14: R = CH$_3$	R_1 = CH$_2$CH = CH$_2$	**31:** R = Cyclohexyl	R_1 = CH$_2$CH$_2$CH$_2$CH$_3$
15: R = CH$_3$	R_1 = CH$_2$-Cyclopropyl	**32:** R = H	R_1 = CH$_2$CH$_3$
16: R = CH$_3$	R_1 = Benzyl	**33:** R = H	R_1 = CH$_2$CH$_2$CH$_3$
17: R = CH$_3$	R_1 = 4-CH$_3$O-Benzyl		

■ MATERIALS AND METHODS

Chemicals. All solvents were purchased from Tianjin Zhi Yuan Regent Co., Ltd. (Tianjin, China). All reagents were purchased from Shanghai Aladdin Biochemical Technology Co., Ltd. (Shanghai, China), Shanghai Macklin Biochemical Co., Ltd. (Shanghai, China), and Adamas Reagent, Ltd. (Shanghai, China). All reagents and solvents were used directly without further purification.

Instruments. The NMR spectra were recorded on a DPX 400 NMR spectrometer (Bruker, Germany) and an ECX-500 NMR spectrometer (JEOL, Japan). The high-resolution mass spectra (HRMS) of the title compounds were recorded on a Thermo Scientific Q Exactive (Thermo Scientific, U.S.). The single-crystal data were collected by a Bruker SMART APEX II (Bruker, Germany). The morphology of the pathogenic bacteria was detected by a FEI Nova Nano SEM 450 (FEI, United States). A Read Max 1900 enzyme-labeled instrument (Shanghai Flash Spectrum Biological Technology Co., Ltd., China) was used to detect the optical density.

General Procedures for Preparing Intermediates. The reaction details of the synthesis intermediates are presented in the Supporting Information.

General Procedures for Preparing Target Compounds 1−33. The synthetic routes for target compounds **1−33** are shown in Scheme 1. Intermediates **C1−C33** (2.0 mmol) were dissolved in methanol (10 mL) and stirred for 15 min. Ammonium molybdate (0.4 mmol) was dissolved in 30% hydrogen peroxide (16.0 mmol),

and the solution was dropped slowly in the reaction flask. After reacting at room temperature for 2−6 h, the mixture was decanted into cooled water and extracted using dichloromethane. The crude products were purified by column chromatography with dichloromethane/methanol (30:1, v/v) to obtain target compounds **1−33**.

In Vitro Antibacterial Activity Test. The in vitro antibacterial activities of compounds **1−33** were evaluated using turbidimetric assays.[21] All of the title compounds dissolved in DMSO were diluted to different concentrations by adding a nutrient broth (NB) medium. Subsequently, *Xoo* or *Xoc* cultures in the logarithmic growth phase were added to the test tubes containing NB medium at a concentration of 1%. After shaking incubation at 180 rpm and 28 °C for 24−48 h, the optical density (OD$_{595}$) of the cultures was estimated at 595 nm using a microplate spectrophotometer. The commercial agents bismerthiazol and thiodiazole copper were formulated into a solution of the same concentration and treated in the same way as the positive controls. The DMSO solution at the same concentration without compounds served as a negative control. The antibacterial EC$_{50}$ values were calculated by GraphPad Prism (version 8.0.2; San Diego, CA) on the basis of the inhibition rate at different concentrations.

3D-QSAR Analysis. The CoMFA models were built using the online web server Cloud 3D-QSAR (http://chemyang.ccnu.edu.cn/ccb/server/cloud3dQSAR/).[22] All molecules (compounds **1−31**) were submitted in SMILES format and separated into a test set (8

compounds) and a training set (23 compounds). The EC_{50} values of the compounds were converted into pEC_{50} and uploaded to the server. The CoMFA analysis was performed using the partial least-squares (PLS) regression approach. The cross-validation correlation coefficient (q^2), non-cross-validated correlation coefficient (r^2), and predictive correlation coefficient (r^2_{pred}), which were used to evaluate the model, were obtained from the Web server. The force field model was visualized using PyMol software (version 1.7.0.0), and the compound with the highest antibacterial activity in the training set was used as the template molecule.

Morphological Change. Cell morphological changes after treatment with compound **33** were observed by scanning electron microscopy.[23] After the bacteria were washed three times, phosphate-buffered saline (PBS) was added to obtain a total volume of 1 mL, and compound **33** dissolved in DMSO was added at concentrations of 2, 5, 25, and 200 mg/L. The same volume of DMSO in 1 mL of PBS served as a negative control. After being shaken at 28 °C for 12 h, the mixture was washed three times with PBS, and 2.5% glutaraldehyde was added to fix the cells for 10 h. PBS was added to wash off the glutaraldehyde, and then the cells were dehydrated with 10%, 30%, 50%, 70%, 90%, and 100% ethanol in turn. The morphological changes were visualized using a scanning electron microscope after the samples were freeze-dried for 4.5 h and coated with gold.

In Vivo Antibacterial Activity Test. The curative and protective activities against BLB were evaluated according to the leaf-cutting method.[24] Commercial agents BT and TC were formulated into a solution of the same concentration and served as positive controls, and the same concentration solution without compounds served as a negative control. Fengyouxiangzhan rice seeds were sown and grown under greenhouse conditions for 5 weeks. The curative activity was evaluated as follows. *Xoo* was inoculated in the NB medium and cultivated until the logarithmic growth phase. The rice leaves were cut 2−3 cm from the leaf tips with sterile surgical scissors, and the rice wounds were immersed in the NB medium with *Xoo* for 15 s. One day after inoculation, a solution containing 200 mg/L of compound **33** was sprayed evenly on the rice leaves until droplets fell, and the positive and negative controls were treated in the same way. The protective activity was evaluated similarly. The solution containing the compound was first evenly sprayed onto the rice leaves until droplets fell, and *Xoo* was inoculated onto the rice the next day. The positive and negative controls were treated in the same way. After inoculation for 14 days, the antibacterial activity could be calculated from the disease index.[12]

The curative and protective activities against BLS were tested by a similar method but using a different inoculation method that was reported in the previous literature with slight modifications.[25] To evaluate the curative activity, *Xoc* cultured to the logarithmic growth phase was used to spot-infiltrate rice leaves with needleless syringes. After 1 day, 0.1% Tween-20 sterile water containing compound **33** (at a concentration of 200 mg/L) was sprayed evenly onto the rice leaves until droplets fell. The positive and negative controls were treated in the same way. For protective activity, the bacteria were inoculated 1 day after spraying compound **33**. The lesion length on the rice was surveyed 14 days later. The equation below illustrates the methods to calculate the curative and protective activities against *Xoc*. In this equation, L indicates the lesion length of the negative control group, and T indicates the lesion length of the treatment group.

$$\text{control efficiencies } E\ (\%) = (L - T)/L \times 100$$

Defensive Enzyme Activities Determination. Compound **33** (200 mg/L) was sprayed on rice plants that grew under greenhouse conditions for 30 days until droplets fell, and the rice plants were inoculated with *Xoc*. The plants were treated with BT and water in the same way as the positive and negative controls, respectively. Rice samples were collected 1, 3, 5, and 7 days after the bacterial infections. The activity of superoxide dismutase (SOD), peroxidase (POD), phenylalanine ammonia-lyase (PAL), and catalase (CAT) was tested using enzyme assay kits (Suzhou Comin Biotechnology Co., Ltd., China).

Determination of Chlorophyll Content. The total chlorophyll (C_t), chlorophyll a (C_a), and chlorophyll b (C_b) contents were tested following a method previously reported.[26]

Proteomics Analysis. *Plant Material and Sampling.* Rice plants grown under greenhouse conditions for 30 days were sprayed with compound **33** (200 mg/L) until wet and infected with *Xoc* after 24 h. The rice samples then were collected, snap-frozen, and stored at −80 °C.

Extraction and Identification of Total Rice Protein. The method of protein extraction and identification was described in our previous work.[27]

Bioinformatics Analysis. Gene ontology (GO) annotations were obtained from the Gene Ontology database (http://www.geneontology.org/), and the GO terms could be divided into three independent categories: molecular functions (MFs), biological processes (BPs), and cellular components (CCs). All differentially expressed proteins (DEPs, fold change > 1.5, *p*-value < 0.05) were mapped in the GO database, and the number of proteins mapped to each GO term was computed. Meanwhile, Kyoto Encyclopedia of Genes and Genomes (KEGG) annotations were performed using the KEGG pathway database (http://www.genome.jp/Pathway).

■ RESULTS AND DISCUSSION

Chemistry. The different substitutes of 4-amino-1,2,4-triazole-3-thiol (**A1−A7**) were prepared by 2-(4-chlorophenoxy)acetohydrazide or carbonothioic dihydrazide. The intermediates **A1−A7** were refluxed with carbon disulfide in a KOH solution of methanol to give 1,2,4-triazolo[3,4-*b*][1,3,4]thiadiazole-6-thiol. Subsequently, target compounds **1−33** were prepared by thioetherification and oxidation reactions. The synthesis methods of the intermediates **C1−C33** and the data for all of the target compounds (melting point, yield, ¹H NMR, ¹³C NMR, and HRMS) are presented in the Supporting Information. A single crystal of compound **20** (CCDC 2041989, Figure S1) was obtained by a slow evaporation of the DCM/EtOH solution and confirmed by X-ray single-crystal diffraction analysis.

In Vitro Antibacterial Activity. The turbidimetric method was used to test the biological activities of target compounds **1−33**. As shown in Table 1, target compounds **1−33** showed good in vitro antibacterial activities against *Xoc* and *Xoo*. The EC_{50} values of compounds **8**, **9**, **11**, **15**, **19**, and **28** against *Xoo* were 0.97, 0.84, 0.74, 0.82, 0.88, and 0.88 mg/L, respectively, which were better than those of TC (90.43 mg/L) and BT (68.37 mg/L). Moreover, the EC_{50} values of compounds **8**, **9**, **11**, and **12** against *Xoc* were 1.58, 1.72, 1.74, and 1.71 mg/L, respectively, which were better than those of TC (97.93 mg/L) and BT (75.59 mg/L).

3D-QSAR Analysis. We built CoMFA models on the basis of the EC_{50} values of compounds **1−31** using the Cloud 3D-QSAR Web server (http://chemyang.ccnu.edu.cn/ccb/server/cloud3dQSAR/). The q^2, r^2, and r^2_{pred} values of the anti-*Xoo* CoMFA model, which were used to evaluate the predictive ability of the model (Figure S2), were 0.9849, 0.6155, and 0.7433, respectively, while the corresponding values of the anti-*Xoc* CoMFA model were 0.9724, 0.6133, and 0.6645, respectively. The high q^2, r^2, and r^2_{pred} values (>0.5) implied that the CoMFA models have good predictive abilities. The residues of the training and test sets in the CoMFA models are presented in Table S1, while the experimental and predicted value distribution maps are shown in Figure 2a and b. All of the residues were close to zero and concentrated near the straight line, illustrating that the CoMFA models might be reliable. As shown in Figure 2c, the 3- and 6-positions of the triazole-thiazole were filled with yellow contours in the steric

Table 1. EC$_{50}$ Values of Target Compounds against *Xanthomonas oryzae* pv. *oryzae* (*Xoo*) and *Xanthomonas oryzae* pv. *oryzicola* (*Xoc*)

compounds	EC$_{50}$ against *Xoo* (mg/L)	EC$_{50}$ against *Xoc* (mg/L)
1	4.10 ± 0.65	8.46 ± 0.58
2	5.03 ± 0.29	7.21 ± 0.63
3	7.14 ± 0.15	4.39 ± 0.32
4	1.26 ± 0.09	3.20 ± 0.47
5	1.13 ± 0.16	2.20 ± 0.16
6	1.38 ± 0.30	2.14 ± 0.11
7	2.30 ± 0.25	5.87 ± 0.30
8	0.97 ± 0.16	1.58 ± 0.22
9	0.84 ± 0.07	1.72 ± 0.13
10	1.24 ± 0.05	2.80 ± 0.19
11	0.74 ± 0.12	1.74 ± 0.10
12	1.05 ± 0.15	1.71 ± 0.04
13	1.15 ± 0.03	2.36 ± 0.12
14	1.08 ± 0.20	2.47 ± 0.29
15	0.82 ± 0.10	2.45 ± 0.29
16	2.72 ± 0.56	2.45 ± 0.13
17	2.56 ± 0.27	3.93 ± 0.29
18	1.28 ± 0.11	2.99 ± 0.63
19	0.88 ± 0.19	2.19 ± 0.10
20	1.04 ± 0.20	3.23 ± 0.09
21	1.31 ± 0.09	3.38 ± 0.22
22	1.14 ± 0.12	5.18 ± 0.10
23	1.39 ± 0.21	8.12 ± 0.11
24	1.56 ± 0.56	3.63 ± 0.15
25	1.78 ± 0.38	7.32 ± 1.01
26	4.39 ± 0.07	14.20 ± 0.55
27	1.73 ± 0.25	4.14 ± 0.31
28	0.88 ± 0.25	3.77 ± 0.20
29	1.87 ± 0.11	4.67 ± 0.19
30	1.26 ± 0.08	6.10 ± 0.51
31	1.71 ± 0.10	6.05 ± 0.62
32[a]	0.61 ± 0.06	1.71 ± 0.12
33[a]	0.59 ± 0.07	1.63 ± 0.16
bismerthiazol	68.37 ± 3.36	75.79 ± 3.66
thiodiazole copper	90.43 ± 2.73	97.34 ± 4.18

[a]Compounds were designed and synthesized on the basis of the CoMFA model. All results are expressed as mean ± SD.

field map, which indicated that the bulky group would not increase the antibacterial activity against *Xoo*. There are blue contours around the side of the ethyl and the oxygen on the sulfone in the electrostatic field map, indicating that benzyl contains electronegative groups more beneficial to exerting anti-*Xoo* activity, as seen by 30 (R = cyclohexyl, 1.26 mg/L) < 19 (R = C$_2$H$_5$, 0.88 mg/L) < 11 (R = CH$_3$, 0.74 mg/L) and 13 (R$_1$ = C$_4$H$_9$, 1.15 mg/L) < 12 (R$_1$ = C$_3$H$_7$, 1.05 mg/L) < 11 (R$_1$ = C$_2$H$_5$, 0.74 mg/L). In the steric field map of Figure 2d, the whole molecule, especially the 3-position, was surrounded by yellow contours, which implied that introducing a bulky group in any position of the molecule was not favorable for anti-*Xoc* activity. Unlike the electrostatic field map of the anti-*Xoo* model, many red contours were distributed around the molecule, which indicated that the electronegative groups were not beneficial for exerting anti-*Xoc* activity; for instance, 30 (R = cyclohexyl, 6.10 mg/L) < 19 (R = C$_2$H$_5$, 2.19 mg/L) < 11 (R = CH$_3$, 1.74 mg/L) and 16 (R$_1$ = Bn, 2.45 mg/L) < 13 (R$_1$ = C$_4$H$_9$, 2.36 mg/L) < 12 (R$_1$ = C$_3$H$_7$, 1.71 mg/L). From the above analysis, we found that introducing the small group at

the 3- and 6-positions will benefit both anti-*Xoo* and anti-*Xoc* activities (Figure 2e and f). Therefore, compounds 32 and 33 with high predicted activities were synthesized and tested for antibacterial activities according to the CoMFA models. The experimental pEC$_{50}$ values of compound 32 against *Xoo* and *Xoc* were 5.5531 and 5.1054, respectively, which were close to the predicted pEC$_{50}$ values (5.5239 and 5.1185, respectively). Additionally, the experimental values of 33 were 5.5947 and 5.1533, respectively, close to the predicted values (5.5020 and 5.1220, respectively). This result indicated that the CoMFA models have good predictive capability and that compounds 32 and 33 designed on the basis of the CoMFA models showed excellent antibacterial activity against the two plant pathogenic bacteria. To evaluate the potential toxicity or mutagenicity of the title compounds, we ran a computational toxicity determination on the ProTox-II web server (https://tox-new.charite.de/protox_II/).[28] The prediction results indicated that compounds 32 and 33 optimized by the CoMFA model have lower oral toxicity (LD$_{50}$ = 2500 mg/kg) and showed no hepatotoxicity, carcinogenicity, immunotoxicity, mutagenicity, or cytotoxicity (Table S2).

Morphological Change. The morphological changes of *Xoc* and *Xoo* are clearly shown in Figure 3. In the negative control group, the cell morphologies were intact with no surface wrinkles. In contrast, the cell surface became wrinkled, and the shape was distorted and even ruptured at 5, 25, and 200 mg/L. When the concentration was reduced to 2 mg/L, the cell surface did not change significantly.

In Vivo Antibacterial Activity. As shown in Table 2 and Figure 4, compound 33 exhibits good protective and curative activities against BLB, with inhibition rates of 49.42% and 47.94%, respectively, which were superior to those of TC (41.51% and 37.97%, respectively). Meanwhile, compound 33 showed good in vivo antibacterial activities against BLS with protective and curative activities of 49.65% and 40.67%, respectively.

Defensive Enzyme Activities Determination. The disease resistance of plants is closely related to defense-related enzyme activities.[29] On the basis of the excellent protective activity against BLB and BLS, we compared some defense enzyme activities of rice after treatment with compound 33. The highest SOD activity of the "33 + *Xoc*" group occurred 1 day after bacterial infection, which was 1.46-, 2.19-, and 2.27-fold higher than that of the "BT + *Xoc*", "CK + *Xoc*", and CK groups, respectively (Figure 5a). Meanwhile, the POD activity of the "33 + *Xoc*" group presented a trend of rising initially and then falling, and was higher than that of the "BT + *Xoc*", "CK + *Xoc*", and CK groups at all experimental time points. The peak value of the POD activity of the "33 + *Xoc*" group at 3 days was 1.94-, 1.91-, and 2.26-fold higher than that of the "BT + *Xoc*", "CK + *Xoc*", and CK groups, respectively (Figure 5b). The PAL and CAT activities of the "33 + *Xoc*" group were not significantly increased as compared to those of the "CK + *Xoc*" and CK groups (Figure 5c and d). Therefore, compound 33 may be able to enhance the disease resistance of rice by improving the activities of rice defense enzymes, especially the SOD and POD activities.

Determination of Chlorophyll Content. Chlorophyll is an important part of photosynthesis. A representative sample was selected at 1 day on the basis of the change in defensive enzyme activities in the experiment. As shown in Figure 5e, the contents of C$_a$, C$_b$, and C$_t$ in the "CK + *Xoc*" group were significantly different from those in the CK group. The
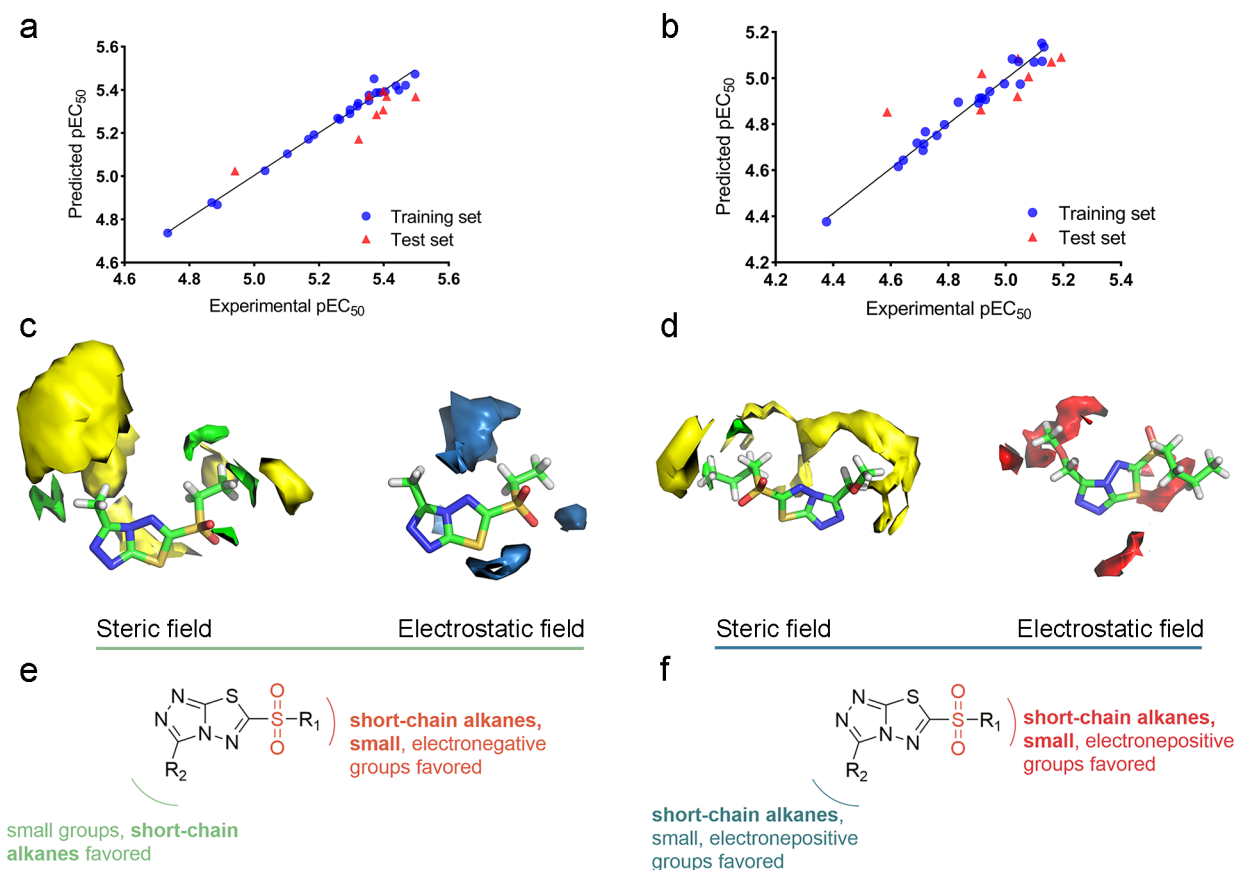
Figure 2. Result of the CoMFA analysis. The correlation between the experimental versus predicted activities of the training and test sets of the anti-*Xoo* model (a) and anti-*Xoc* model (b). The field contour maps of the CoMFA models based on the antibacterial activity against *Xoo* (c) and *Xoc* (d). The relationship between the structure and antibacterial activity against *Xoo* (e) and *Xoc* (f).
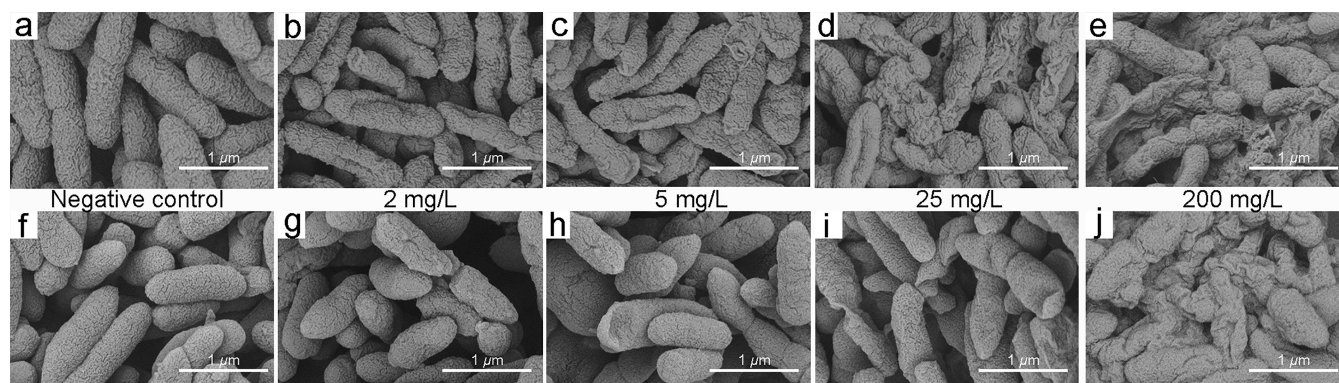

Figure 3. Effect of compound **33** on the cell morphology of *Xanthomonas oryzae* pv. *oryzae* (a−e) and *Xanthomonas oryzae* pv. *oryzicola* (f−j).

Table 2. Protective and Curative Activities In Vivo of Compound 33 against Bacterial Diseases at 200 mg/L

treatment	bacterial leaf blight[a]		bacterial leaf streak[a]	
	curative activity (%)	protective activity (%)	curative activity (%)	protective activity (%)
33	47.94 ± 3.72 a	49.42 ± 2.98 a	40.67 ± 5.74 a	49.65 ± 5.06 a
bismerthiazol	43.71 ± 3.66 ab	40.09 ± 4.79 b	36.25 ± 3.85 ab	38.89 ± 3.22 b
thiodiazole copper	37.97 ± 4.52 b	41.51 ± 3.88 b	28.80 ± 3.71 b	44.28 ± 4.76 ab

[a]All results are expressed as mean ± SD. Statistical analysis was conducted by ANOVA method under the condition of equal variances assumed ($P > 0.05$) and equal variances not assumed ($P < 0.05$). Different lowercase letters indicate activity values with significant differences among different treatment groups at $P < 0.05$.

chlorophyll contents (C_a, C_b, and C_t) were significantly higher in the "**33** + *Xoc*" group than in the "CK + *Xoc*" and CK
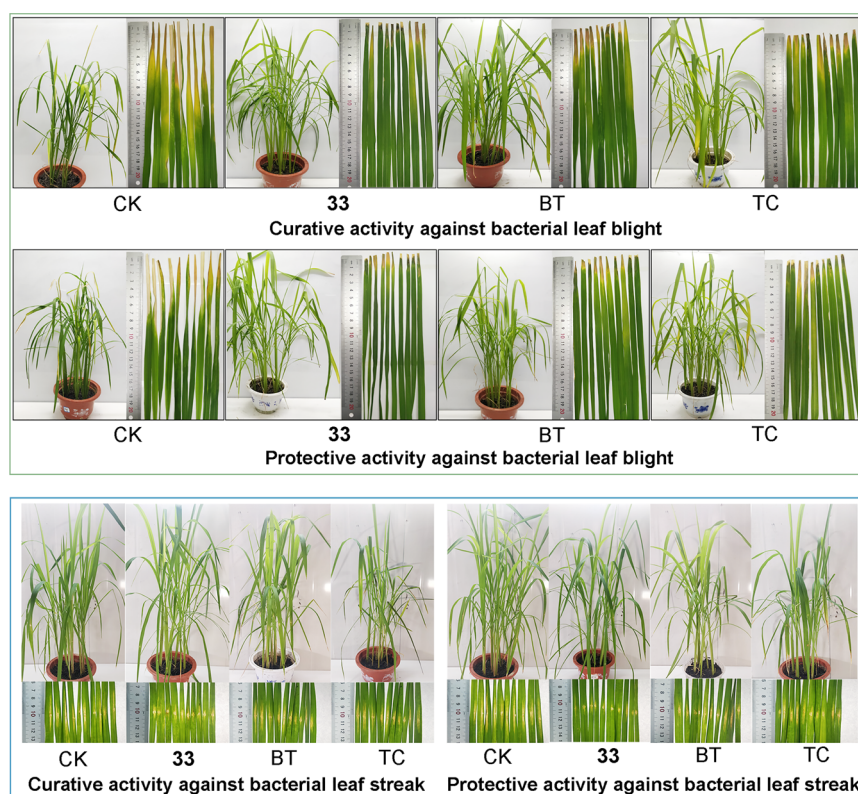
Figure 4. Curative and protective activities of compound **33** against rice bacterial leaf blight and bacterial leaf streak at 200 mg/L. CK, negative control; BT, bismerthiazol; TC, thiodiazole copper.

groups. The results imply that the chlorophyll contents of rice decreased with bacterial infection but that compound **33** may inhibit such a decrease in chlorophyll content.

Proteomics Analysis. A total of 1530 proteins were identified from both the "**33** + *Xoc*" and the "CK + *Xoc*" groups. Among them, 1323 proteins were identified from the "**33** + *Xoc*" group, and 1155 proteins were identified from the "CK + *Xoc*" group. The number of uniquely expressed proteins was 207 and 375 in the "CK + *Xoc*" and "**33** + *Xoc*" groups, respectively. The DEPs between the "**33** + *Xoc*" group and the "CK + *Xoc*" group included 172 upregulated proteins (red points) and 65 downregulated proteins (blue points), as illustrated in the volcanic map (Figure S3).

Biofunctional Analysis. The GO enrichment analysis of DEPs (*p*-value ≤ 0.05) in the two groups was classified into three GO categories: CCs, BPs, and MFs (Figure S4). The main CCs included the membrane, chloroplast, thylakoid, cytoplasm, cell, nucleus, intracellular, ribosome, cytosol, apoplast, mitochondrion, nucleosome, and extracellular region. In the MFs, proteins were enriched in oxidoreductase activity, peroxidase activity, RNA binding, DNA binding, zinc ion binding, NAD binding, nucleic acid binding, ATP binding, GTPase activity, hydrolase activity, GTP binding, metal ion binding, heme binding, and calcium ion binding. The DEPs in BPs were mainly enriched in the metabolic process, photosynthesis, defense response to bacterium, chlorophyll biosynthetic process, protein folding, translation, response to oxidative stress, glycolytic process, hydrogen peroxide catabolic process, rRNA processing, carbohydrate metabolic process, cell redox homeostasis, response to stress, carotenoid biosynthetic process, and defense response. The above data indicate that compound **33** can regulate plant cell components and key molecular functions. Moreover, defense-related GO terms, such as photosynthesis, the hydrogen peroxide catabolic process, the chlorophyll biosynthetic process, the defense response to bacterium, the response to oxidative stress, the response to stress, and the defense response, were enriched in BPs. This result illustrated that compound **33** might regulate defense-related proteins, which are closely associated with the elevation of POD, SOD, and chlorophyll, to improve disease resistance in rice.

KEGG Classification Analysis. To determine the mode of action triggered by compound **33**, possible biological pathway analyses were performed using the KEGG database. As illustrated in Table 3 and Figure 6, a total of 14 proteins were enriched in the photosynthesis pathway. Among these proteins, eight proteins were upregulated, and six proteins did not change. Compound **33** mainly upregulated proteins related to photosystem II (IDs: Q8H4P7_ORYSJ, Q943W1_ORYSJ, Q7F2L7_ORYSJ, and Q6Z1 V5_ORYSJ), photosystem I (IDs: PSAH_ORYSJ, Q84PB5_ORYSJ, and Q84PB4_OR-YSJ), and electron transport (ID: PLAS_ORYSJ), which involve photon capture and electron transport from photosystem II (PSII) to the photosystem I (PSI) reaction center. In plant disease defense responses, photosynthesis often plays an important role.[30] Bacterial stress can cause a decrease in photosynthesis, and plant genotypes that can maintain photosynthesis often present higher disease resistance under stress conditions.[31,32] The induction of plant defense is energy-intensive, and the synthesis of defense compounds demands photoassimilates as a carbon source.[33] This increases the demand for photosynthesis in plants that are infected by pathogens. Compound **33** can increase the chlorophyll contents and upregulate multiple proteins in PSII, electron
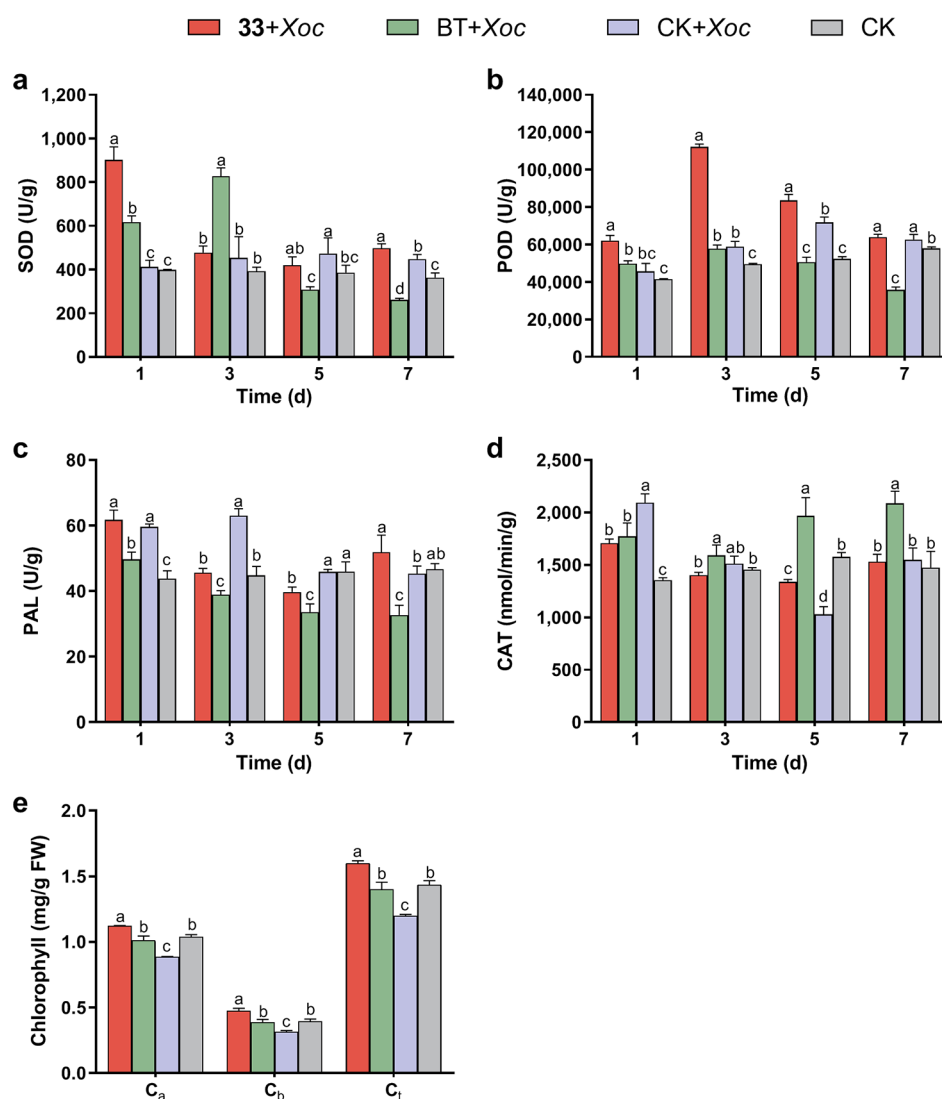
Figure 5. Effect of compound **33** on defense enzymes and chlorophyll in rice: (a) superoxide dismutase (SOD), (b) peroxidase (POD), (c) phenylalanine ammonia-lyase (PAL), and (d) catalase (CAT). (e) Changes in chlorophyll a (C_a), chlorophyll b (C_b), and total chlorophyll content (C_t). The values are the means and standard deviation of three independent experiments. Different lowercase letters indicate values with significant differences among different treatment groups according to a one-way ANOVA ($P < 0.05$).

Table 3. Differentially Expressed Proteins Involved in the Photosynthetic Pathway

ID	protein names	gene names	regulated[a]
PSAH_ORYSJ	photosystem I reaction center subunit VI	PSAH GOS5	1
PLAS_ORYSJ	plastocyanin	PETE	1
FENR3_ORYSJ	ferredoxin-NADP reductase	Os07g0147900	0
Q7F2L7_ORYSJ	cytochrome b559 subunit alpha	psbE	1
Q6Z1V5_ORYSJ	cytochrome b559 subunit beta	psbF	1
FENR1_ORYSJ	ferredoxin-NADP reductase	LFNR1	0
Q7XVG7_ORYSJ	ferredoxin	Os04g0412200	0
Q84PB5_ORYSJ	PSI-K	Os07g0148900	1
Q84NW1_ORYSJ	Os07g0513000 protein	Os07g0513000	0
Q84PB4_ORYSJ	chloroplast photosystem I reaction center subunit II-like protein	Os08g0560900	1
Q10LV7_ORYSJ	Os03g0333400 protein	LOC_Os03g21560	0
Q943W1_ORYSJ	Os01g0501800 protein	Os01g0501800	1
Q8H4P7_ORYSJ	photosystem II	OJ1470_H06.117	1
Q2QWN3_ORYSJ	Os12g0189400 protein	LOC_Os12g08770	0

[a]1 means significant upregulation. 0 means no significant difference between the treatment and control groups.

Figure 6. Differentially expressed proteins involved in the photosynthetic pathway. The upregulated proteins are represented by red in this pathway, whereas the unchanged proteins are represented by blue.

transport, and PSII. These results indicate that the capture of photons, excitation of electrons, and electron transport in photosynthesis were promoted by compound **33** and that the disease resistance of rice was improved. Infection by pathogenic bacteria often increases the level of reactive oxygen species (ROS). Excessive ROS will inhibit photosynthesis, cause oxidative damage, and damage DNA, proteins, and lipids.[34] Plants cope with ROS by generating antioxidant enzymes. After treatment with compound **33**, the content of antioxidant enzymes such as POD and SOD increased abundantly, which was beneficial for scavenging ROS. Meanwhile, inhibition of photosynthesis caused by excess ROS will be reduced by upregulating photosynthesis-related protein expression, and chloroplast damage will be alleviated. Among these proteins, plastocyanin (ID: PLAS_ORYSJ) is not only involved in electron transport but also binds copper ions and reduces the formation of hydroxyl radicals to improve the antioxidant activity of the plant.[35,36] The experimental results suggest that compound **33** may upregulate the protein involved in the main process of the light reactions to decrease photosynthesis inhibition under bacterial stress and improve the antioxidant capacity of the plant by regulating plastocyanin. These results are consistent with the elevation of the defense enzyme activities and chlorophyll content.

In summary, we designed and synthesized a series of novel 6-sulfonyl-1,2,4-triazolo[3,4-b][1,3,4]thiadiazole derivatives, and their antibacterial activities were evaluated. Two CoMFA models were established to analyze the structure−activity relationship of the compounds, and compounds **32** and **33**,

with higher antibacterial activities, were designed and synthesized on the basis of the models. In addition, the antibacterial activities of **33** are closely related to the regulation of the activities of defense-related enzymes, the chlorophyll content, and photosynthesis. Compound **33** was also consistent in upregulating the expression of defense responses and photosynthesis-related proteins, which may improve the disease resistance of rice. Therefore, compound **33** can be used as a lead compound to develop novel antibacterial agents and provide ideas to study the mechanism of action.

■ ASSOCIATED CONTENT

ⓢ Supporting Information

The Supporting Information is available free of charge at https://pubs.acs.org/doi/10.1021/acs.jafc.1c01204.

> Syntheses, characterizations, and physical and analytical data of intermediates **C1−C33** and target compounds **1−33** (PDF)
>
> All identified proteins (XLSX)

■ AUTHOR INFORMATION

Corresponding Authors

Liansheng Zang − *State Key Laboratory Breeding Base of Green Pesticide and Agricultural Bioengineering, Key Laboratory of Green Pesticide and Agricultural Bioengineering, Ministry of Education, Center for Research and Development of Fine Chemicals, Guizhou University, Guiyang 550025, People's Republic of China*; Phone: +86-

851083620521; Email: lsz0415@163.com; Fax: +86-0851-83622211

Baoan Song − *State Key Laboratory Breeding Base of Green Pesticide and Agricultural Bioengineering, Key Laboratory of Green Pesticide and Agricultural Bioengineering, Ministry of Education, Center for Research and Development of Fine Chemicals, Guizhou University, Guiyang 550025, People's Republic of China;* ⊙ orcid.org/0000-0002-4237-6167; Email: basong@gzu.edu.cn

Authors

Sikai Wu − *State Key Laboratory Breeding Base of Green Pesticide and Agricultural Bioengineering, Key Laboratory of Green Pesticide and Agricultural Bioengineering, Ministry of Education, Center for Research and Development of Fine Chemicals, Guizhou University, Guiyang 550025, People's Republic of China*

Jing Shi − *State Key Laboratory Breeding Base of Green Pesticide and Agricultural Bioengineering, Key Laboratory of Green Pesticide and Agricultural Bioengineering, Ministry of Education, Center for Research and Development of Fine Chemicals, Guizhou University, Guiyang 550025, People's Republic of China*

Jixiang Chen − *State Key Laboratory Breeding Base of Green Pesticide and Agricultural Bioengineering, Key Laboratory of Green Pesticide and Agricultural Bioengineering, Ministry of Education, Center for Research and Development of Fine Chemicals, Guizhou University, Guiyang 550025, People's Republic of China*

Deyu Hu − *State Key Laboratory Breeding Base of Green Pesticide and Agricultural Bioengineering, Key Laboratory of Green Pesticide and Agricultural Bioengineering, Ministry of Education, Center for Research and Development of Fine Chemicals, Guizhou University, Guiyang 550025, People's Republic of China;* ⊙ orcid.org/0000-0001-7843-371X

Complete contact information is available at:
https://pubs.acs.org/10.1021/acs.jafc.1c01204

Author Contributions

[†]S.W. and J.S. contributed equally to this work.

Notes

The authors declare no competing financial interest.

■ ABBREVIATIONS USED

^{1}H NMR, ^{1}H nuclear magnetic resonance; ^{13}C NMR, ^{13}C nuclear magnetic resonance; HRMS, high-resolution mass spectrometry; DMSO, dimethyl sulfoxide; Xoo, *Xanthomonas oryzae* pv. *oryzae*; Xoc, *Xanthomonas oryzae* pv. *oryzicola*; BT, bismerthiazol; TC, thiodiazole copper; EC_{50}, 50% effective concentration; 3D-QSAR, three-dimensional quantitative structure−activity relationship; CoMFA, comparative molecular field analysis; SOD, superoxide dismutase; POD, peroxidase; PAL, phenylalaninammonialyase; CAT, catalase; C_t, total chlorophyll; C_a, chlorophyll a; C_b, chlorophyll b; DEPs, differentially expressed proteins; MFs, molecular functions; BPs, biological process; CCs, cellular components; PSI, photosystem I; PSII, photosystem II; ROS, reactive oxygen species

■ REFERENCES

(1) Seck, P. A.; Diagne, A.; Mohanty, S.; Wopereis, M. C. Crops that feed the world 7: Rice. *Food Secur.* **2012**, *4*, 7−24.

(2) Li, C. X.; Zhang, J. G.; Ren, Z. Y.; Xie, R.; Yin, C. X.; Ma, W. H.; Zhou, F.; Chen, H.; Lin, Y. J. Development of 'multi-resistance rice' by assembly of herbicide, insect and disease resistance genes with a transgene stacking system. *Pest Manage. Sci.* **2021**, *77*, 1536−1547.

(3) Sundaram, R. M.; Chatterjee, S.; Oliva, R.; Laha, G. S.; Cruz, C. V.; Leach, J. E.; Sonti, R. V. Update on bacterial blight of rice: fourth international conference on bacterial blight. *Rice* **2014**, *7*, 12.

(4) Yuan, T.; Li, X. H.; Xiao, J. H.; Wang, S. P. Characterization of *Xanthomonas oryzae*-responsive *cis*-acting element in the promoter of rice race-specific susceptibility gene *Xa13*. *Mol. Plant* **2011**, *4*, 300−309.

(5) Jiang, N.; Yan, J.; Liang, Y. L.; He, Z. Z.; Wu, Y. T.; Zeng, Q.; Liu, X. J.; Peng, J. H. Resistance genes and their interactions with bacterial blight/leaf streak pathogens (*Xanthomonas oryzae*) in rice (*Oryza sativa* L.)—an updated review. *Rice* **2020**, *13*, 3.

(6) Zhu, X. F.; Xu, Y.; Peng, D.; Zhang, Y.; Huang, T. T.; Wang, J. X.; Zhou, M. G. Detection and characterization of bismerthiazol-resistance of *Xanthomonas oryzae* pv. *oryzae*. *Crop Prot.* **2013**, *47*, 24−29.

(7) Zhou, X.; Feng, Y. M.; Qi, P. Y.; Shao, W. B.; Wu, Z. B.; Liu, L. W.; Wang, Y.; Ma, H. D.; Wang, P. Y.; Li, Z.; Yang, S. Synthesis and docking study of *N*-(cinnamoyl)-*N*-(substituted)acryloyl hydrazide derivatives containing pyridinium moieties as a novel class of filamentous temperature-sensitive protein Z inhibitors against the intractable *Xanthomonas oryzae* pv. *oryzae* infections in rice. *J. Agric. Food Chem.* **2020**, *68*, 8132−8142.

(8) Xu, W. M.; Han, F. F.; He, M.; Hu, D. Y.; He, J.; Yang, S.; Song, B. A. Inhibition of tobacco bacterial wilt with sulfone derivatives containing an 1,3,4-oxadiazole moiety. *J. Agric. Food Chem.* **2012**, *60*, 1036−1041.

(9) Wang, P. Y.; Zhou, L.; Zhou, J.; Wu, Z. B.; Xue, W.; Song, B. A.; Yang, S. Synthesis and antibacterial activity of pyridinium-tailored 2,5-substituted-1,3,4-oxadiazole thioether/sulfoxide/sulfone derivatives. *Bioorg. Med. Chem. Lett.* **2016**, *26*, 1214−1217.

(10) Chen, J. X.; Luo, Y. Q.; Wei, C. Q.; Wu, S. K.; Wu, R.; Wang, S. B.; Hu, D. Y.; Song, B. A. Novel sulfone derivatives containing a 1,3,4-oxadiazole moiety: design and synthesis based on the 3D-QSAR model as potential antibacterial agent. *Pest Manage. Sci.* **2020**, *76*, 3188−3198.

(11) Su, S. H.; Zhou, X.; Liao, G. P.; Qi, P. Y.; Jin, L. H. Synthesis and antibacterial evaluation of new sulfone derivatives containing 2-aroxymethyl-1,3,4-oxadiazole/thiadiazole moiety. *Molecules* **2017**, *22*, 61−64.

(12) Xiang, J.; Liu, D. Y.; Chen, J. X.; Hu, D. Y.; Song, B. A. Design and synthesis of novel 1,3,4-oxadiazole sulfone compounds containing 3,4-dichloroisothiazolylamide moiety and evaluation of rice bacterial activity. *Pestic. Biochem. Physiol.* **2020**, *170*, 104695.

(13) Karegoudar, P.; Prasad, D. J.; Ashok, M.; Mahalinga, M.; Poojary, B.; Holla, B. S. Synthesis, antimicrobial and anti-inflammatory activities of some 1,2,4-triazolo[3,4-*b*][1,3,4]-thiadiazoles and 1,2,4-triazolo[3,4-*b*][1,3,4]thiadiazines bearing trichlorophenyl moiety. *Eur. J. Med. Chem.* **2008**, *43*, 808−815.

(14) Qing, Z. L.; Zhang, X. Synthesis and fungicidal activity of 3-aryl-6-(*p*-chlorobenzoylamino)-*S*-triazolo[3,4-*b*]-1,3,4-thiadiazoles. *Chin. J. Org. Chem.* **2008**, *28*, 1483−1486.

(15) Lin, L.; Liu, H.; Wang, D. J.; Hu, Y. J.; Wei, X. H. Synthesis and biological activities of 3,6-disubstituted-1,2,4-triazolo-1,3,4-thiadiazole derivatives. *Bull. Chem. Soc. Ethiop.* **2018**, *31*, 481−489.

(16) Badr, S. M.; Barwa, R. M. Synthesis of some new [1,2,4]triazolo[3,4-*b*][1,3,4]thiadiazines and [1,2,4]triazolo[3,4-b]-[1,3,4] thiadiazoles starting from 5-nitro-2-furoic acid and evaluation of their antimicrobial activity. *Bioorg. Med. Chem.* **2011**, *19*, 4506−4512.

(17) Plech, T.; Wujec, M.; Kosikowska, U.; Malm, A.; Kaproń, B. Studies on the synthesis and antibacterial activity of 3,6-disubstituted 1,2,4-triazolo[3,4-*b*]1,3,4-thiadiazoles. *Eur. J. Med. Chem.* **2012**, *47*, 580−584.

(18) Lv, X. Y.; Yang, L.; Fan, Z. J.; Bao, X. P. Synthesis and antimicrobial activities of novel quinazolin-4(*3H*)-one derivatives containing a 1,2,4-triazolo[3,4-*b*][1,3,4]thiadiazole moiety. *J. Saudi Chem. Soc.* **2018**, *22*, 101−109.

(19) Zhao, B.; Fan, S. J.; Fan, Z. J.; Wang, H. X.; Zhang, N. L.; Guo, X. F.; Yang, D. Y.; Wu, Q. F.; Yu, B.; Zhou, S. Discovery of pyruvate kinase as a novel target of new fungicide candidate 3-(4-methyl-1,2,3-thiadiazolyl)-6-trichloromethyl-[1,2,4]-triazolo-[3,4-*b*][1,3,4]-thiadizole. *J. Agric. Food Chem.* **2018**, *66*, 12439−12452.

(20) Kamboj, V. K.; Kapoor, A.; Jain, S. Synthesis, antimicrobial, and antioxidant screening of aryl acetic acid incorporated 1,2,4-triazolo-1,3,4-thiadiazole derivatives. *J. Heterocycl. Chem.* **2019**, *56*, 1376−1382.

(21) Wang, X.; Li, P.; Li, Z. N.; Yin, J.; He, M.; Xue, W.; Chen, Z. W.; Song, B. A. Synthesis and bioactivity evaluation of novel arylimines containing a 3-aminoethyl-2-[(*p*-trifluoromethoxy)-anilino]-4(*3H*)-quinazolinone moiety. *J. Agric. Food Chem.* **2013**, *61*, 9575−9582.

(22) Wang, Y. L.; Wang, F.; Shi, X. X.; Jia, C. Y.; Wu, F. X.; Hao, G. F.; Yang, G. F. Cloud 3D-QSAR: a web tool for the development of quantitative structure-activity relationship models in drug discovery. *Briefings Bioinf.* **2020**, No. bbaa276.

(23) Yi, C. F.; Chen, J. X.; Wei, C. Q.; Wu, S. K.; Wang, S. B.; Hu, D. Y.; Song, B. A. *α*-Haloacetophenone and analogues as potential antibacterial agents and nematicides. *Bioorg. Med. Chem. Lett.* **2020**, *30*, 126814.

(24) Wang, C. L.; Xu, A. B.; Gao, Y.; Fan, Y. L.; Liang, Y. T.; Zheng, C. K.; Sun, L. Q.; Wang, W. Q.; Zhao, K. J. Generation and characterisation of Tn5-tagged *Xanthomonas oryzae* pv. *oryzae* mutants that overcome *Xa23*-mediated resistance to bacterial blight of rice. *Eur. J. Plant Pathol.* **2009**, *123*, 343−351.

(25) Zou, H. S.; Yuan, L.; Guo, W.; Li, Y.-R.; Che, Y. Z.; Zou, L. F.; Chen, G. Y. Construction of a Tn5-tagged mutant library of *Xanthomonas oryzae* pv. *oryzicola* as an invaluable resource for functional genomics. *Curr. Microbiol.* **2011**, *62*, 908−916.

(26) Gan, X. H.; Hu, D. Y.; Wang, Y. J.; Yu, L.; Song, B. A. Novel trans-ferulic acid derivatives containing a chalcone moiety as potential activator for plant resistance induction. *J. Agric. Food Chem.* **2017**, *65*, 4367−4377.

(27) Yang, A. M.; Yu, L.; Chen, Z.; Zhang, S. X.; Shi, J.; Zhao, X. Z.; Yang, Y. Y.; Hu, D. Y.; Song, B. A. Label-free quantitative proteomic analysis of chitosan oligosaccharide-treated rice infected with southern rice black-streaked dwarf virus. *Viruses* **2017**, *9*, 115.

(28) Banerjee, P.; Eckert, A. O.; Schrey, A. K.; Preissner, R. ProTox-II: a webserver for the prediction of toxicity of chemicals. *Nucleic Acids Res.* **2018**, *46*, 257−263.

(29) Zhang, G. Q.; Feng, J. T.; Han, L. R.; Zhang, X. Antiviral activity of glycoprotein GP-1 isolated from *Streptomyces kanasensis* ZX01. *Int. J. Biol. Macromol.* **2016**, *88*, 572−577.

(30) Hu, H.; Sheng, L.; Zhang, G. Z.; Gu, Q.; Zheng, K. F. Influence of bacterial leaf blight on the photosynthetic characteristics of resistant and susceptible rice. *J. Phytopathol.* **2018**, *166*, 547−554.

(31) Khojasteh, M.; Khahani, B.; Taghavi, M.; Tavakol, E. Identification and characterization of responsive genes in rice during compatible interactions with pathogenic pathovars of *Xanthomonas oryzae*. *Eur. J. Plant Pathol.* **2017**, *151*, 141−153.

(32) Kerchev, P. I.; Fenton, B.; Foyer, C. H.; Hancock, R. D. Plant responses to insect herbivory: interactions between photosynthesis, reactive oxygen species and hormonal signalling pathways. *Plant, Cell Environ.* **2012**, *35*, 441−453.

(33) Göhre, V.; Jones, A. M. E.; Sklenář, J.; Robatzek, S.; Weber, A. P. Molecular Crosstalk between PAMP-triggered immunity and photosynthesis. *Mol. Plant-Microbe Interact.* **2012**, *25*, 1083−1092.

(34) Shi, K.; Gao, Z.; Shi, T. Q.; Song, P.; Ren, L. J.; Huang, H.; Ji, X. J. Reactive oxygen species-mediated cellular stress response and lipid accumulation in oleaginous microorganisms: the state of the art and future perspectives. *Front. Microbiol.* **2017**, *8*, 793.

(35) Zhou, X. T.; Wang, F.; Ma, Y. P.; Jia, L. J.; Liu, N.; Wang, H. Y.; Zhao, P.; Xia, G. X.; Zhong, N. Q. Ectopic expression of SsPETE2, a plastocyanin from *Suaeda salsa* improves plant tolerance to oxidative stress. *Plant Sci.* **2018**, *268*, 1−10.

(36) Höhner, R.; Pribil, M.; Herbstová, M.; Lopez, L. S.; Kunz, H. H.; Li, M.; Wood, M.; Svoboda, V.; Puthiyaveetil, S.; Leister, D.; Kirchhoff, H. Plastocyanin is the long-range electron carrier between photosystem II and photosystem I in plants. *Proc. Natl. Acad. Sci. U. S. A.* **2020**, *117*, 15354−15362.